Design of frontal longitudinal for enhancement in crashworthiness performance

Design of frontal longitudinal for enhancement in crashworthiness performance

Samer Fakhri Abdulqadir[1], Alaseel Bassam[2,3], M N M Ansari[4], and A Topa[5,6]

[1] Department of Mechanical Engineering, University of Anbar, Iraq.
[2] Mechanical Engineering Department, Universiti Tenaga National (UNITEN), 43000 Kajang, Malaysia.
[3] Department of Administration, State company of Phosphate, Anbar, Iraq.
[4] Institute of Power Engineering, Universiti Tenaga Nasional, 43000 Kajang, Selangor,Malaysia.
[5] Ocean and Ship Technology Group, Institute of Transportation Infrastructure, Universiti Teknologi PETRONAS, Perak, 32610, Malaysia.
[6] Department of Maritime Technology, Faculty of Ocean Engineering Technology and Informatics, Universiti Malaysia Terengganu, Kuala Terengganu, 21300, Malaysia.

Corresponding author: ansari@uniten.edu.my; ansari.uniten@gmail.com

Abstract. The increase in the number of vehicles due to increase in population leads to an increase in the number of accidents. To find a design that keeps occupants as safe as possible by enhancing the energy absorption capabilities and hence decreasing the number of fatalities is taking place. Non-linear finite element is used in this study to predict new design performance and to compare with other conventional S-shaped designs. It was shown that the proposed design increased the specific energy absorption (SEA) by 265% in comparison with the conventional S-Shaped frame design with octagonal geometries and increased in SEA 16% of the S-Shaped with foam filled-square cross-sectional. In this study, the specific energy absorption will take in consideration the energy absorber used is made of mild steel.

1. Introduction

Collisions cause thousands of people either killed or injured around the world every year [1], [2]. In Malaysia, the road network had been developed by 650% and the length of the road reached to 71,814 km from 1971 to 2005 due to the population growth and the number of vehicles [3]. According to (Royal Malaysian Police 2011), the number of fatalities due to accidents has increased by 1.8% (2009: 6745 to 6872 in 2010) [4]. the (World Health Organization 2009) has predicted that more than 1.2 million people die due to road accident each year and the number of injuries about 20 to 50 million. To enhance the crashworthiness of the structure, the proposed design must support an offset 40% collisions as well as the direct one. Australian New Car Assessment Program ANCAP (2006)[5] demonstrated that about 35% of all vehicle collisions were oblique impacts as shown in figure 1 below. Therefore, around 70% of all accidents happen in the front car whether in the direct or oblique collisions. So, it is important to concentrate on how to design frontal car structures that able to absorb the most impact energy during collisions in different directions.

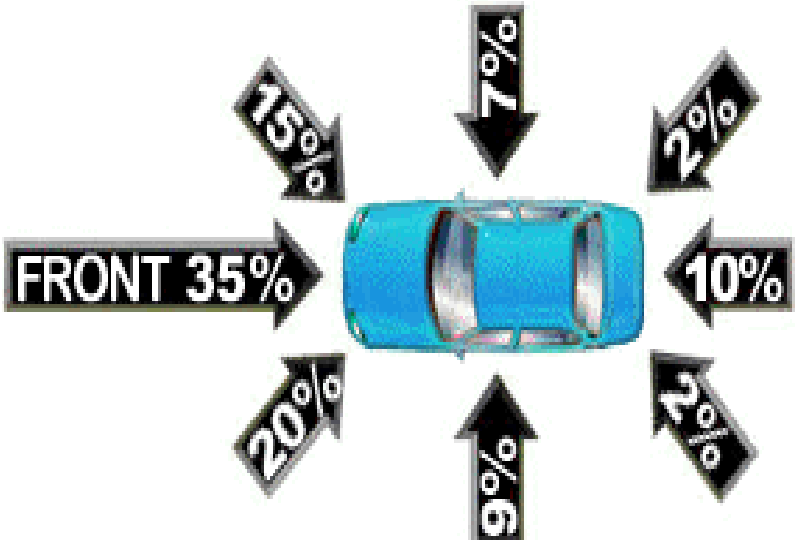

Figure 1. Percentages of vehicle impact direction [4].

Researchers and manufacturers paid their attention to occupants' safety, which became the most critical design objective in ground vehicles [6]. To save and protect vehicle's occupants, the design of structures must be able to absorb as much as possible energy caused by collision due to plastic deformation and keep car compartment away from severe deformation and decrease the intrusion of the vehicle. To carry out these conditions, the design should take into consideration that both longitudinal must work together during a collision, this enables the structure to absorb enough energy and keeps occupants safer. The decreasing of absorbed energy comes when one or both longitudinal is not loaded axially and hence the bending will happen. The proposed design tries to achieve two roles, the first one is getting higher absorbed energy and the second one is in oblique or 40 percent offset collision, the energy absorbed by the longitudinal should be almost as same as in a direct collision. Witteman (1993) stated that it is important to design a stiff longitudinal structure to be able to dissipate enough energy when loaded partially in overlap collision.

The structure should be strengthened to prevent or decrease the bending during collisions which will decrease in the amount of absorbed energy. The structure should be flexible when loaded axially to reduce excessive-high deceleration [3]. Many studies [3], [7], [8] have been implemented using different cross-section tubes subjected to direct and 40 per cent offset dynamic loading. These studies have found that the hexagonal tube was the best choice depending on multi-criteria decision making (MCDM) process. The parameters selected were included energy absorption (EA) and crash force efficiency (CFE). Samer [3] has studied the using of the hexagonal tube as a longitudinal absorber subjected to dynamic load with different directions. The study was compared with the conventional S-shaped used in the car. The study has concluded that using thin-walled hexagonal tube has superior performance than conventional one since it has higher energy absorption capability and lower acceleration within acceptable limits.

2. Finite element modeling

ABAQUS (non-linear finite element) has been employed to study the thin-walled hexagonal structure. The finite element was used to predict the behavior of the structure under dynamic loading. The hexagonal tube was modelled by using 4-node shell continuum (S4R) element along the thickness direction of the tube. When the aluminum foam is incorporated, the foam was modelled using 8-noded continuum elements with reduced integration techniques with incorporated hourglass control. The size of the mesh used was 5mm. The contact interaction between all parts was general contact algorithm. Coefficient of friction was incorporated between the foam and tube wall and it was set at 0.2 [9]–[11].

Plates were modelled as a rigid body. Moving plate (striker) was permitted to move axially along the structure while other translational and rotations degree of freedom were fixed. The impact velocity of the striker on the structure was set as 56km/h with a mass of 275kg (figure 3). The velocity was used according to the New Car Assessment Program (NCAP) by the National Highway Traffic Safety Administration (NHTSA). The study has taken a mass with 25 % of the compact car (1100) kg. Each longitudinal was assumed to absorb an equivalent kinetic of 275kg mass since the maximum absorbed energy by the two longitudinal is less than 50% [12].

3. Materials

3.1. Steel

A36 steel material was used in this study to simulate the structure. The A36 steel is a very common material, cheaper, most available and high energy absorption capability used in design as energy absorption. A36 was modelled as per Johnson-Cook constitutive isotropic model. It's more accurate to take in consideration the strain rate varies since this material is strain rate dependent [13], [14]. Material characterizations are combined as in Equation 1. [15].

$$\sigma_T = \left[A + B\left(\varepsilon_{eff}^{p}\right)^{N}\right]\left(1 + C\ln\frac{\dot{\varepsilon}_{eff}^{p}}{\dot{\varepsilon}_0}\right)\left[1 - \left(\frac{T - T_0}{T_{melt} - T_0}\right)^{M}\right] \quad (1)$$

Where σ_T is the dynamic flow stress.
The ε_{eff}^{p} is the effective plastic strain
$\dot{\varepsilon}_{eff}^{p}$ is the effective plastic strain rate.
$\dot{\varepsilon}_0^{p}$ is a reference strain rate,
$T_{melt}$is the melting temperature, and
A, B, N, M and C are material parameters.
whereas T_0 is the transition temperature and it is usually taken as the room temperature of 293-297 ° Kelvin [16], [17]. The parameters of Johnson-Cook are given in Table 1[18].

Table 1. Summary of parameters for A36 steel[19].

Parameter	Value	Description
A	146.7 MPa	Material parameter
B	896.9 MPa	Material parameter
N	0.320	Strain power coefficient
C	0.033	Material parameter
M	0.323	Temperature power coefficient
$\dot{\varepsilon}_0$	1.0 sec-1	Reference strain rate
r	7850 kg/m3	Density
Tm	1773 °K	Melting Temperature
Cp	486 J/kg-°K	Specific Heat

3.2. Aluminum foam

The CRUSHABLE FOAM and the CRUSHABLE FOAM HARDENING options are assigned in the ABAQUS/Explicit software package to consider the plastic aluminium foam behaviour. This option based on the foam model by Deshpande and Fleck [20]. The foam properties used in this study are listed in Table 2.

Table 2. Summary of parameters for aluminum foam model[9].

r_f(kg/m^3)	s_p (MPa)	a	a_2 (MPa)	b	g	e_D
534	12.56	2.12	1544	3.680	1.00	1.6206

4. Results and Dissection

4.1. Full overlap collision

In this type of collision, both absorber members are loaded axially. Figure 2 shows the structure of the longitudinal member. The SEA which is equal to the energy absorbed by the structure divided by both structure masses in addition to the foam mass. The structure is shown in Figure 3. The thickness used in this study was 2mm. The structure was fixed from one end and the free end subjected to the striker of 1100 kg which represents an average car with two occupants and luggage [20], with striker velocity of 54km/h. Foam-filled steel enhances the energy absorption and gives the folding more stability and hence more folded, which increases the energy absorption and the crash force efficiency (CFE).

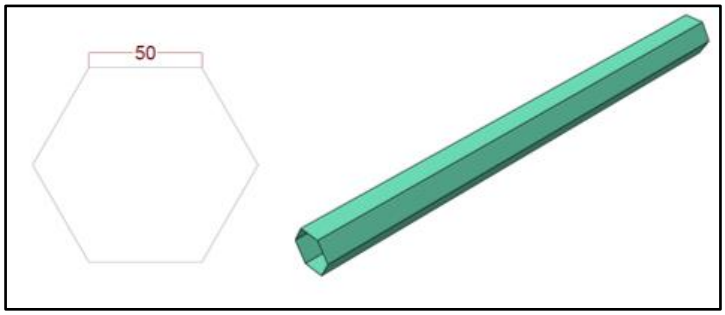

Figure 2. structure designs two and three dimensions.

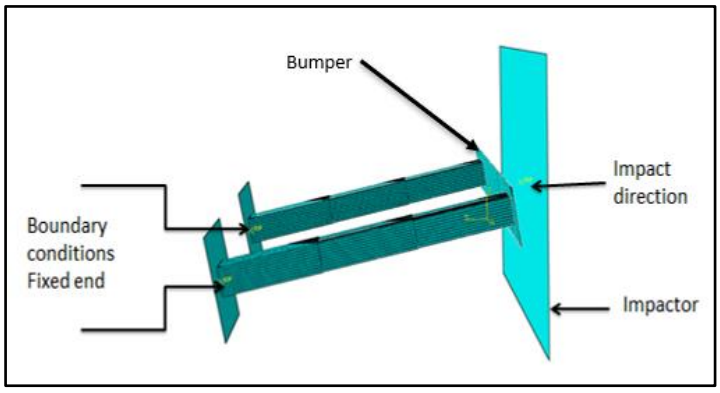

Figure 3. Finite element modeling and boundary condition for the proposed design.

The specific energy absorption (SEA) diagram is shown in Figure 4 which represents the function of displacement. The figure has been demonstrated that the highest specific energy absorption was 4.4 (kJ/kg). In this case, both members are loaded axially. From the Figure (4), the curve starts with almost no energy absorbed until reach 10 mm which represents the impactor hitting the bumper without absorber, when the impactor reaches the absorbers, the absorbed energy starts to increase with the displacement and the energy is directly proportional with the displacement. The curve is almost linear and reaches the maximum displacement no rebound has occurred.

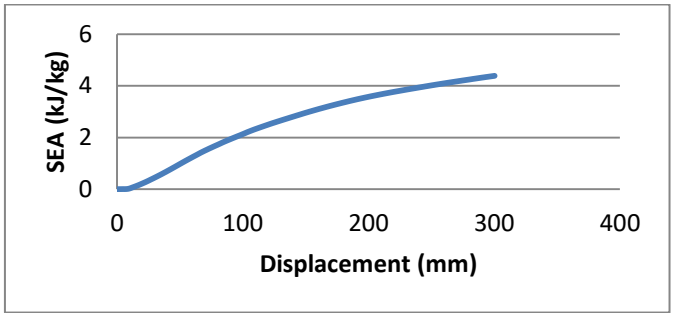

Figure 4. Specific Energy absorption (SEA) – displacement for foam aluminum filled steel.

Figure 5 represents the force-displacement curve which begins to rise with low steep until it reaches (25 kN) which represents the impactor hitting the bumper before reaching the absorber. When the impactor reaches the absorbers, the curve starts to rise rapidly with a very short time until it reaches the maximum value at (160kN), representing the force needed to form the first fold of each absorber. The absorber after forming the first fold starts to be less stiff, so the force needed to form more folds will be less. The force begins to decelerate gradually with more time, which is preferable to avoid high rapid deceleration less serious injuries.

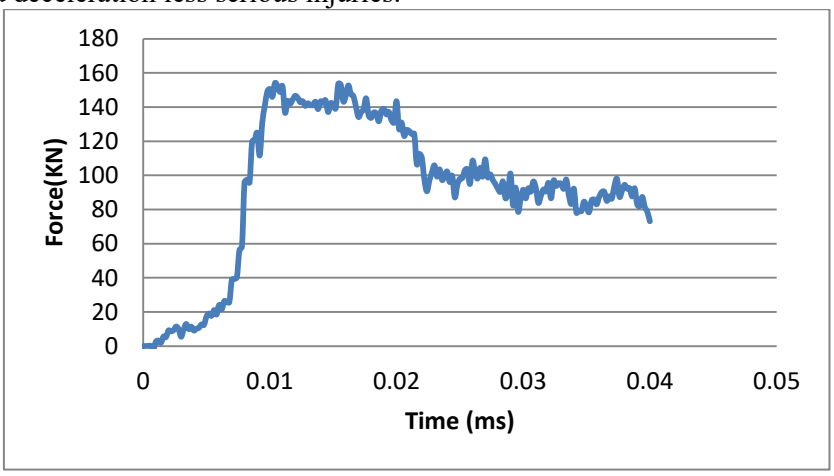

Figure 5. Force - displacement curve for the proposed design.

Figure 6 represents the deceleration-time curve. The deceleration behaves as a result of the force. The figure shows that the maximum deceleration is at high peak force when the first fold is formed. The maximum acceleration is 16 g, this magnitude is acceptable according to [21] and it's much lower than the permissible level. The basic levels of HIC for different occupant sizes are shown in Table 3 below::

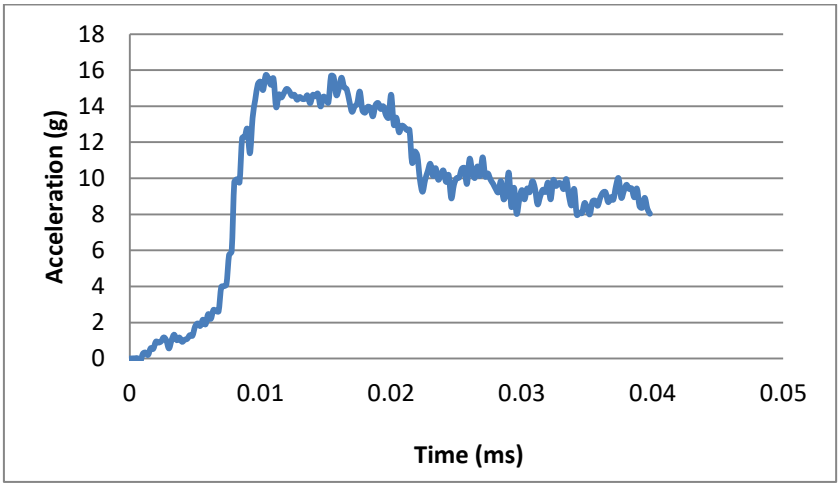

Figure 6. Acceleration-displacement curve for a proposed design.

Table 3. HIC level for different Occupant Sizes[21].

Dummy Type	Mid-Sized Male	Small Female	6 Year Old Child	3 Year Old Child	12 Month Old Infant
Existing/Proposed HIC Limit	1000	1000	1000	900	660

According to the table, the acceptable acceleration level is 60 g. The acceleration below this limit means that the structure is safer and recommended and vehicle occupants will be at a lower risk level. Equation 2 shows the parameters affecting HIC.

$$HIC = \left\{ \left[\frac{1}{t_2 - t_1} \int_{t_1}^{t_2} a(t)dt \right]^{2.5} (t_2 - t_1) \right\}_{max} \quad (2)$$

Where t_1 and t_2 refer to any two random times during the acceleration pulse [21] a is a resultant head acceleration [22].

4.2. Forty per cent (40%) offset collision

The purpose of using 40 per cent offset collision is to assess the proposed design when subjected to this type of loading. In this collision, one of the longitudinal members is loaded axially and the other one is unloaded. When the impactor starts to collide the structure, first it will reach the bumper. The bumper will absorb a small amount of energy comparing with the absorber. The impactor continues to move on towards the structure for 110 mm as in figure 7. When the impactor starts to contact the stiff absorber, the energy starts to increase rapidly with a short time, and it increases as displacement increased. The purpose of using 40 per cent offset collision is to assess the proposed design when subjected to this type of loading. In this collision, one of the longitudinal members is loaded axially and the other one is unloaded. When the impactor starts to collide the structure, first it will reach the bumper. The bumper will absorb a small amount of energy comparing with the absorber. The impactor continues to move on towards the structure for 110 mm as in figure 7. When the impactor starts to contact the stiff absorber, the energy starts to increase rapidly with a short time, and it increases as displacement increased.

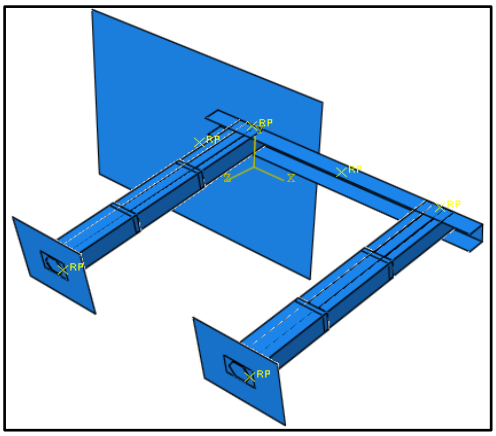

Figure 7. Proposed design subjected to 40 percent offset loading.

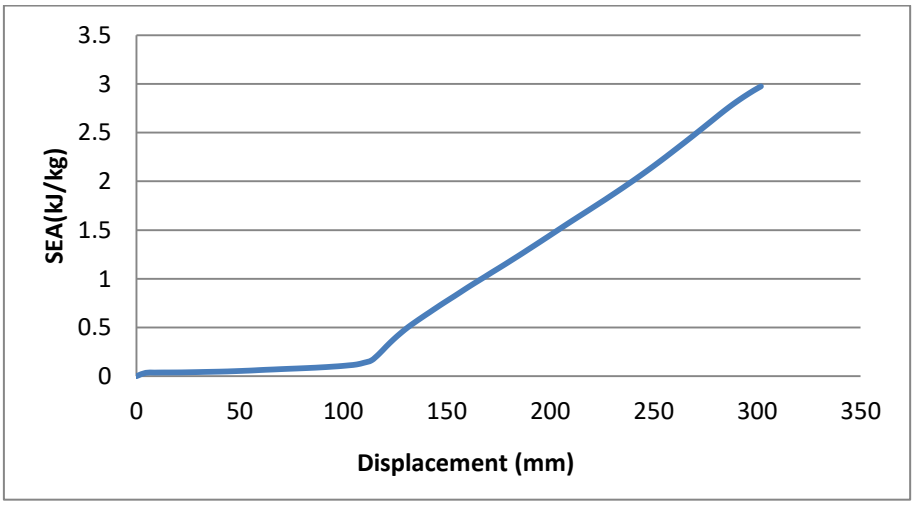

Figure 8. Specific Energy absorption (SEA) – displacement for foam aluminum filled steel in an offset collision (40%).

In the case of 40 percent offset crash, the rigid body has impacted the vehicle with a velocity of 54 km/h. In the 40 percent offset overlap. From figure 8 it can be said that the SEA of the structures is up to 3 (KJ/Kg). In an overlap collision, the vehicle started to rotate due to non-symmetrical loading, and this leads to non-symmetrical deformation mode, reactions, displacements and velocities of the two energy absorbers. Figure 9 represents the force-time curve for both left and right frontal longitudinal. The maximum force level of loaded side is nearly 152 KN after 10 ms, after that time the curve fluctuates below that level due to buckling until it reaches 68.6KN at time of 40 ms, while the unloaded side shows increasing slowly with low force level until the end of simulation and the force at that time is about 24 KN.

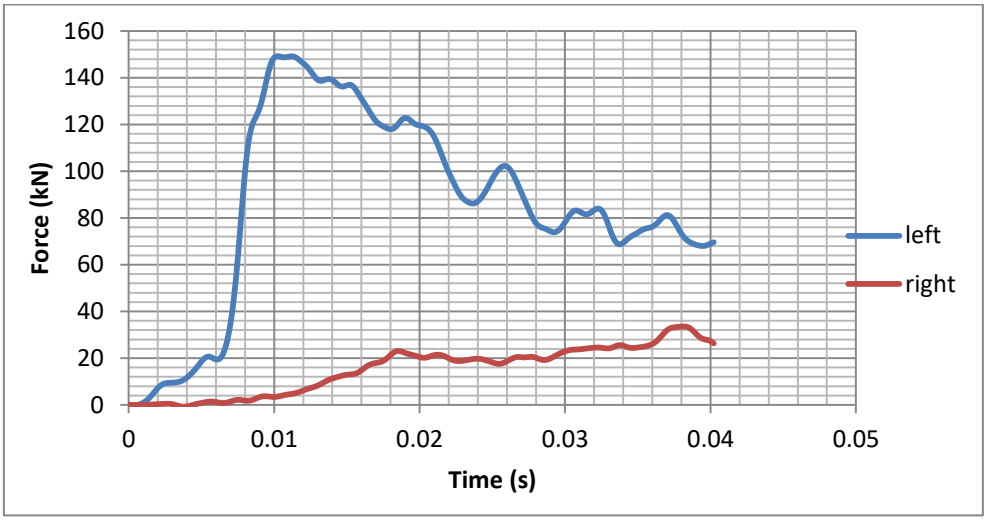

Figure 9. Forces of left and right longitudinal of foam-filled steel with 40 percent offset crash.

The deceleration curve of the 40 percent offset crash for both left and right absorber is plotted in Figure 10. The same difference can be seen in the force figure. The peak deceleration in the left absorber was 15.2 g at 10 ms, after that the deceleration fluctuates and decreases until it reaches 7.1 g at 40 ms, due to the buckling. The right absorber starts to increase due to increasing the force until it reaches the peak value of 2.5 g at 40 ms.

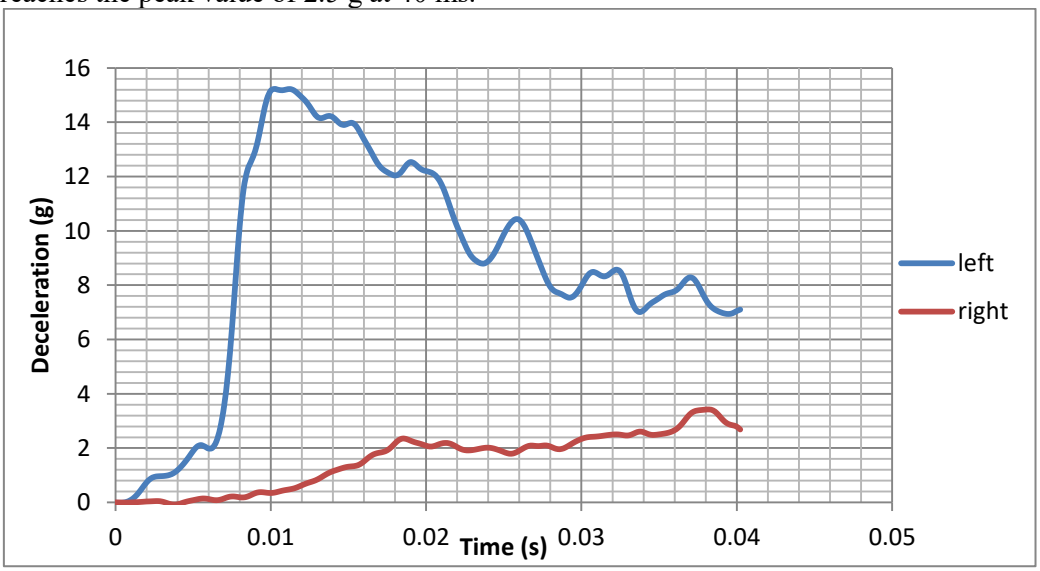

Figure 10. Deceleration of left and right longitudinal of foam-filled steel with 40 percent offset crash.

5. Structure design comparison

Ahmed Elmarakbi et al. [23] used the conventional design (S-shaped) for both aluminum and steel. The study included the different cross-section and different inner stiffening as shown in Figure 11 below. The maximum specific energy absorption that has got were in these types type 2, type 3, type 7 (selected design), type 8 and type 10 (1.377, 1.342, 1.549, 1.411 and 1.656 (KJ/Kg) when using octagonal with different inner stiffening. From the other hand, another study done by Zhang and Saigal [24] they designed S-Shaped structure with different square cross-sectional shapes.

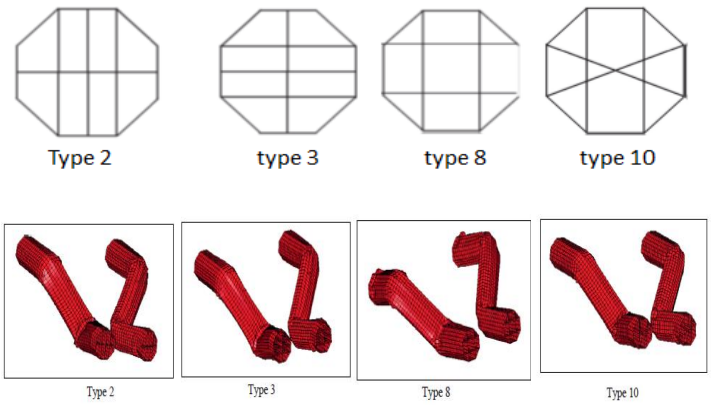

Figure 11. Two and three-dimension of the S-Shaped designs.

Table 4. SEA of different profiles with proposed design.

Profile	Name	SEA (KJ/Kg
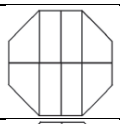	S-Shaped type 2	1.377
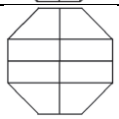	S-Shaped type 3	1.342
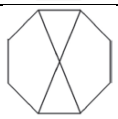	S-Shaped type 7 (selected design)	1.549
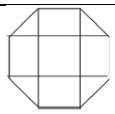	S-Shaped type 8	1.411
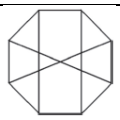	S-Shaped type 10	1.656
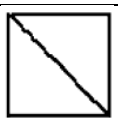	Square S-Shaped	3.8
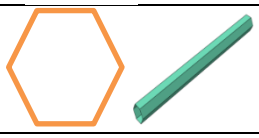	proposed design	4.4

They stated that the highest SEA is 1.375 KJ/Kg and when the foam incorporated with their design, the highest SEA is 3.8 kJ/kg. they concluded that the foam-filled structure increases the SEA. Figures 12 show the comparison of different S-shaped design and proposed design.

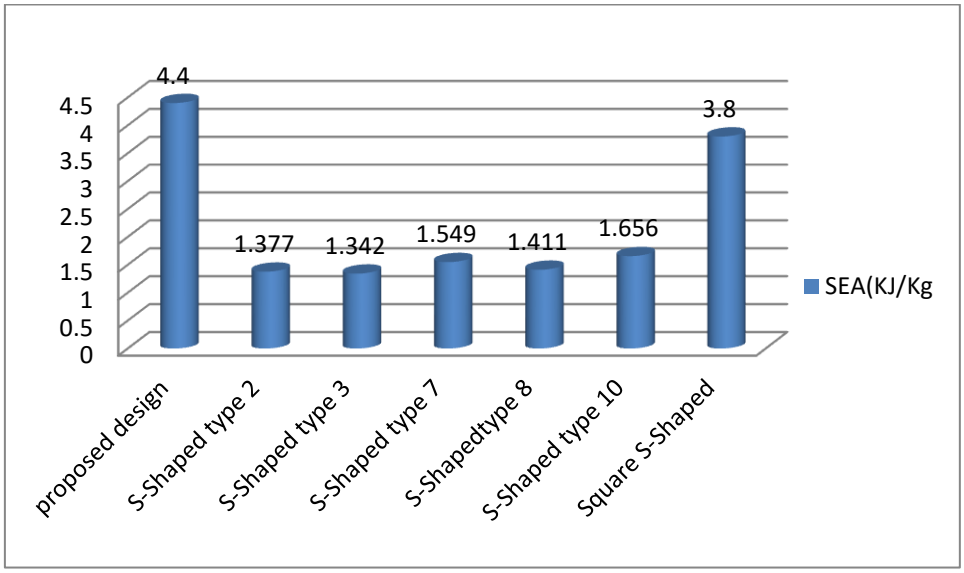

Figure 12. Specific energy absorption of different S-Shaped designs and proposed design.

6. Conclusion and Future Work

This research fulfilled two goals, at first a new design subjected to full overlap car collisions was evaluated and the second was the behavior assessment of 40 percent offset overlap impact on the proposed energy absorber. The proposed design is compared with other conventional S-shaped designs with different cross-sectional geometries used in the car. Numerical simulations were done by using ABAQUS. Results presented in this study were showed that the SEA of the frontal longitudinal members can be enhanced by using the proposed design. The results showed that the SEA of the proposed design was higher than other designs and the peak force and hence the acceleration is much lower than critical recommended by HIC. It can be concluded that the proposed design enhances the energy absorption and it increases the SEA by 265% of the S-Shaped designs with different octagonal geometries and increases SEA by 16% of the S-Shaped design when incorporated the foam filled-square cross-sectional. For 40 percent offset collision, the simulations showed good results the SEA is about 3(kJ/kg) which represented 68% of the full overlap and the deceleration is much lower than critical level.

Author's contribution

Samer Fakhri Abdulqadir[1]-Idea & concept generation**,** first draft and manuscript writing, simulation data collection, analyses of data,; **Alaseel Bassam**[2,3] - simulation and interpretation of the data, manuscript editing. **M N M Ansari**[4] suggestion and advise on the interpretation, presentation of the data and manuscript editing; **Ameen topa**[5,6] - simulation and analytical tools application, manuscript editing.

References

[1] A. A. Mohammed, K. Ambak, A. M. Mosa, and D. Syamsunur, "A Review of the Traffic Accidents and Related Practices Worldwide," Open Transp. J., vol. 13, no. 1, pp. 65–83, 2019, doi: 10.2174/1874447801913010065.
[2] Y. Maqbool, "Road safety and Road Accidents : An Insight Road safety and Road Accidents : An Insight," Int. J. Inf. Comput. Sci., vol. 6, no. 4, pp. 93–105, 2019.
[3] S. F. Abdulqadir, "Design a new energy absorber longitudinal member and compare with S-shaped design to enhance the energy absorption capability," Alexandria Eng. J., vol. 57, no. 4, pp. 3405–3418, 2018, doi: 10.1016/j.aej.2018.07.012.
[4] S. I. Ao, X. Huang, and O. Castillo, Lecture Notes in Electrical Engineering: Preface, vol. 70

LNEE, no. July. 2011.
[5] "CrashTest.com." [Online]. Available: http://www.crashtest.com/search_caf.php?src=mountains&uid=www5ea081acc95756.21598985&abp=1&country=MY&query=CarCrash&afdToken=3B1g-UGgKbOLnQTdwvTMZ2f6nL1Y3GkUmIqpon-b0D2e-_jslfg6AZ69rMFsG7uHbHI7OViuXl7Q_7QQycVxegqCwXIGXebTEbV64LeEUGw. [Accessed: 23-Apr-2020].
[6] M. M. Trivedi, T. Gandhi, and J. McCall, "Looking-in and looking-out of a vehicle: Computer-vision-based enhanced vehicle safety," IEEE Trans. Intell. Transp. Syst., vol. 8, no. 1, pp. 108–120, 2007, doi: 10.1109/TITS.2006.889442.
[7] F. Tarlochan, F. Samer, A. M. S. Hamouda, S. Ramesh, and K. Khalid, "Design of thin wall structures for energy absorption applications: Enhancement of crashworthiness due to axial and oblique impact forces," Thin-Walled Struct., vol. 71, pp. 7–17, 2013, doi: 10.1016/j.tws.2013.04.003.
[8] . S. F., "Improvement of Energy Absorption of Thin Walled Hexagonal Tube Made of Magnesium Alloy By Using Trigger Mechanisms," Int. J. Res. Eng. Technol., vol. 02, no. 10, pp. 173–180, 2013, doi: 10.15623/ijret.2013.0210025.
[9] Z. Ahmad and D. P. Thambiratnam, "Dynamic computer simulation and energy absorption of foam-filled conical tubes under axial impact loading," Comput. Struct., vol. 87, no. 3–4, pp. 186–197, 2009, doi: 10.1016/j.compstruc.2008.10.003.
[10] A. G. Olabi, E. Morris, M. S. J. Hashmi, and M. D. Gilchrist, "Optimised design of nested circular tube energy absorbers under lateral impact loading," Int. J. Mech. Sci., vol. 50, no. 1, pp. 104–116, 2008, doi: 10.1016/j.ijmecsci.2007.04.005.
[11] A. G. Olabi, E. Morris, M. S. J. Hashmi, and M. D. Gilchrist, "Optimised design of nested oblong tube energy absorbers under lateral impact loading," Int. J. Impact Eng., vol. 35, no. 1, pp. 10–26, 2008, doi: 10.1016/j.ijimpeng.2006.11.007.
[12] S. Alkhatib, "Sami Emad Alkhatib-201103668-Thesis," no. January, 2018.
[13] X. Kong, Q. Fang, J. Zhang, and Y. Zhang, "Numerical prediction of dynamic tensile failure in concrete by a corrected strain-rate dependent nonlocal material model," Int. J. Impact Eng., vol. 137, no. October 2019, 2020, doi: 10.1016/j.ijimpeng.2019.103445.
[14] Z. Liao, X. Yao, L. Zhang, M. Hossain, J. Wang, and S. Zang, "Temperature and strain rate dependent large tensile deformation and tensile failure behavior of transparent polyurethane at intermediate strain rates," Int. J. Impact Eng., vol. 129, no. January, pp. 152–167, 2019, doi: 10.1016/j.ijimpeng.2019.03.005.
[15] J. Dean, C. S. Dunleavy, P. M. Brown, and T. W. Clyne, "Energy absorption during projectile perforation of thin steel plates and the kinetic energy of ejected fragments," Int. J. Impact Eng., vol. 36, no. 10–11, pp. 1250–1258, 2009, doi: 10.1016/j.ijimpeng.2009.05.002.
[16] V. Kumar, L. Singh, and A. K. Tripathi, "Reliability analysis of safety-critical and control systems: A state-of-the-art review," IET Softw., vol. 12, no. 1, pp. 1–18, 2018, doi: 10.1049/iet-sen.2017.0053.
[17] A. Sedky and A. T. AlMotasem, "Fluctuation-Induced Excess Conductivity and Infrared Spectra in Y Doped BSCCO Superconductors," J. Mater. Appl., vol. 8, no. 1, pp. 41–49, 2019, doi: 10.32732/jma.2019.8.1.41.
[18] C. W. Isaac and O. Oluwole, "Numerical modelling of the effect of non-propagating crack in circular thin-walled tubes under dynamic axial crushing," Thin-Walled Struct., vol. 115, no. February, pp. 119–128, 2017, doi: 10.1016/j.tws.2017.02.012.
[19] C. Duan, H. Yu, Y. Cai, and Y. Li, "Finite element simulation and experiment of chip formation during high speed cutting of hardened steel," Appl. Mech. Mater., vol. 29–32, no. 5, pp. 1838–1843, 2010, doi: 10.4028/www.scientific.net/AMM.29-32.1838.
[20] V. S. Deshpande and N. A. Fleck, "Isotropic constitutive models for metallic foams," J. Mech. Phys. Solids, vol. 48, no. 6, pp. 1253–1283, 2000, doi: 10.1016/S0022-5096(99)00082-4.
[21] E. S. R. S. Michael Kleinberger, "Development of Improved Injury Criteria for the

Assessment," no. September, 1998.
[22] B. McHenry, "Head injury criterion and the ATB," ATB Users' Gr., no. February, pp. 5–8, 2004.
[23] A. Elmarakbi, Y. X. Long, and J. MacIntyre, "Crash analysis and energy absorption characteristics of S-shaped longitudinal members," Thin-Walled Struct., vol. 68, pp. 65–74, 2013, doi: 10.1016/j.tws.2013.02.008.
[24] C. Zhang and A. Saigal, "Crash behavior of a 3D S-shape space frame structure," J. Mater. Process. Technol., vol. 191, no. 1–3, pp. 256–259, 2007, doi: 10.1016/j.jmatprotec.2007.03.093.